Environmental Research 206 (2022) 112617

Contents lists available at ScienceDirect

Environmental Research

journal homepage: www.elsevier.com/locate/envres

# Development of label-free fluorescent biosensor for the detection of kanamycin based on aptamer capped metal-organic framework

Shanshan Liu *, Yanmei Chen, Zhijun Ruan, Junqi Lin **, Wen Kong ***

*Hubei Key Laboratory of Processing and Application of Catalytic Materials, College of Chemistry and Chemical Engineering, Huanggang Normal University, Huanggang, 438000, China*

ARTICLE INFO

*Keywords:*
Fluorescence
ZIF-8
Aggregation-induce emission
Kanamycin
Aptasensor
Antibiotic

ABSTRACT

The abuse of antibiotics has caused serious threat to human health, so it is of great significance to develop a simple and sensitive method for the detection of trace residues of antibiotics in the environment and food. Herein, a novel label-free fluorescent biosensing platform based on the fluorescence change of aptamers-capped zeolitic imidazolate framework-8 (ZIF-8) @ 2,2′,2″,2‴-((ethene-1,1,2,2-tetrayltetrakis (benzene-4,1-diyl)) tetrakis (oxy)) tetraacetic acid (TPE) through ATP-assisted competitive coordination reaction was designed for such an end. ZIF-8@TPE/Aptamer (Apt) emits strong fluorescence at 425 nm in HEPES buffer due to the aggregation induced luminescence properties of TPE molecules in confined state. Once kanamycin was added, the conformation of aptamer capped on the surface of ZIF-8@TPE changes because of the specific recognition of kanamycin with aptamer, leading to the collapse of ZIF-8 and release of TPE, accompanied with a dramatic decrease of fluorescence intensity. Under the optimal conditions, a good correlation was obtained between the fluorescence intensity of ZIF-8@TPE/Apt and the concentration of kanamycin ranging from 10 to $10^3$ ng/mL with a detection limit of 7.3 ng/mL. The satisfactory analytical performance of the assay for kanamycin detection suggests good prospect for its application in food safety analysis.

## 1. Introduction

As a broad-spectrum aminoglycoside antibiotic, kanamycin could effectively inhibit the biological activity of most gram-negative bacteria (e.g., *E. coli,* Salmonella, Bacillus pneumoniae, proteus) by disrupting protein synthesis through mRNA misread (Ben et al., 2019; Ramezani et al., 2016; Zhou et al., 2020). Because of its excellent antibacterial activities, it is widely used in clinic, aquaculture, agriculture and so on (Qu et al., 2016; Zhang et al., 2020; Jiang et al., 2018). However, the abuse of kanamycin would lead to the enrichment of kanamycin in ecosystems, and eventually become a threat pose inevitable threats to human health through the food chain, causing diseases such as ototoxicity, nephrotoxicity, hepatotoxicity, and neuromuscular block (Kuehn et al., 2019; Yao et al., 2019; He et al., 2019). To avoid the occurrence of such medical problems and the emergence of super-resistant bacteria, China has established maximum residue limits for kanamycin in ecological environment and animal-origin food (Jiang et al., 2019). It is hence of great significance to develop a sensitive method for accurate detection of kanamycin.

Up to now, various analytical methods based on colorimetry (Hou et al., 2018; Son et al., 2019), electrochemistry (Cheng et al., 2020; Tian et al., 2020; Zhou et al., 2019), photoelectrochemistry (Zeng et al., 2021) enzyme-linked immunosorbent assay (ELISA) (He et al., 2016), high performance liquid chromatography (Chen et al., 2009), capillary electrophoresis (Chen et al., 2018), gas chromatography-mass spectrometry (Preu et al., 1998), and surface-enhanced Raman scattering (Jiang et al., 2019) have been proposed for the detection of kanamycin. Although these assays have their own superiority, they suffer from drawbacks. For example, the colorimetric approach is limited in sensitivity, whereas the electrochemical methods are inseparable from tedious electrode modification and accompanied with inferior stability, which may affect detection accuracy. ELISA requires the involvement of expensive antibodies. The other techniques are mostly time consuming as well as require complicated operation and sophisticated equipment. Hence, it is urgent to develop strategies that are simple and sensitive for kanamycin detection. As an alternative, fluorescent methods that are

* Corresponding author.
** Corresponding author.
*** Corresponding author.
*E-mail addresses:* liushanshanlhl@163.com (S. Liu), linjunqi@hgnu.edu.cn (J. Lin), kongwen@hgnu.edu.cn (W. Kong).

https://doi.org/10.1016/j.envres.2021.112617
Received 28 October 2021; Received in revised form 22 November 2021; Accepted 21 December 2021
Available online 27 December 2021

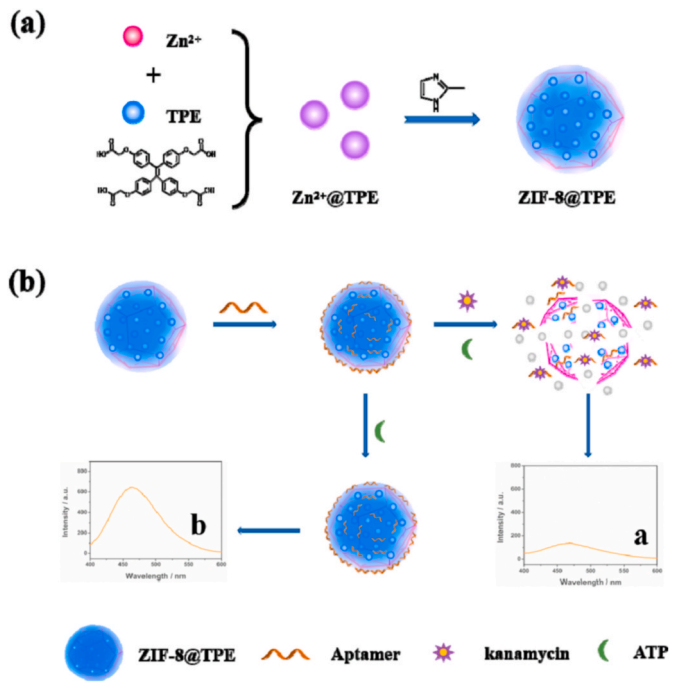


**Scheme 1.** Schematic of (a) ZIF-8@TPE synthesis procedure and (b) Schematic of label-free fluorescent aptasensor for kanamycin detection based on ZIF-8@TPE/Apt.

simple, stable, and economic have been widely applied in biosensing. There are two key factors affecting the performance of a fluorescent biosensor, viz. robust fluorescent material, and reliable recognition element.

As a new type of fluorescent molecule, aggregation-induce emission (AIE) fluorochromes have been widely used in optoelectronic devices (Zeng et al., 2019; Li et al., 2019), as well as chemical sensing (Peng et al., 2020; Wang et al., 2014) and biological imaging (Ma et al., 2021). Different from the traditional fluorochromes with aggregation-caused quenching, AIE fluorochromes show weak fluorescence in the dissolved state or random state, but the fluorescence intensity is dramatically increased in the aggregated or confined state (Cai et al., 2017). The zeolitic imidazolate framework-8 (ZIF-8) with porous structure is an attractive material for molecule encapsulation (Shi et al., 2020). When the AIE fluorochromes were encapsulated in ZIF-8, the composite material would show intense fluorescence due to the confined state of AIE fluorochromes by the rigid framework. What's more, the rigid metal-organic frameworks could be decomposed by changing the pH of the solution or introducing competitive ligands, enabling it a promising fluorochromes carrier (Liang et al., 2015; Gu et al., 2021). As screened by systematic evolution of ligands by exponential enrichment (SELEX), aptamers, which are artificial oligonucleotides, could specifically bind to certain targets with high affinity through their specific three-dimensional structure (Yan et al., 2016; Gu et al., 2019; Wang et al., 2019). As promising recognition entities, aptamers possess many merits, such as precise repetition, high synthesis yield, wide range of targets, high chemical stability, robust affinity and specificity, and ease for modification and labeling (Feng et al., 2018; Lan et al., 2017). Hence, aptamers have attracted much attention in the field of biosensors for the detection of various targets (Xi et al., 2021; Liu et al., 2020). In addition, the negatively charged aptamers could be absorbed on the surface of metal-organic frameworks with π-electron-rich ligands through π-π stacking and electrostatic interactions (Wang et al., 2020). Therefore, aptamers are suitable to act as the recognition capping units for the encapsulation of fluorochromes in metal-organic frameworks to facilitate the control of fluorescence intensity.

Herein, we report the development of a novel aptamers-capped ZIF-8@2,2′,2″,2‴-((ethene-1,1,2,2-tetrayltetrakis (benzene-4,1-diyl)) tetrakis (oxy)) tetraacetic acid (TPE)-based fluorescent sensing strategy for ultrasensitive detection of kanamycin using ATP-assisted competitive coordination reactions (Scheme 1b). The prepared ZIF-8@TPE synthesized by a one-step reaction (Scheme 1a) exhibits intense fluorescence due to the confined state of the encapsulated TPE. In the presence of ATP, there is the competitive coordination reaction between ATP and $Zn^{2+}$, accompanied by the collapse of ZIF-8 framework and the release of TPE, leading to a significant decrease of ZIF-8@TPE fluorescence. When the negatively charged aptamer cover on the surface of ZIF-8@TPE, the resulted ZIF-8@TPE/Apt could exist stably in the ATP-containing solution. With the addition of kanamycin, the aptamers would combine with kanamycin to form a hairpin structure and detach from ZIF-8@TPE, causing fluorescence intensity to decrease. On this basis, a cost-effective and sensitive assay for kanamycin sensing is developed. The biosensor exhibits satisfactory analytical performance for the detection of kanamycin, showing bright prospect in the sensing of antibodies.

## 2. Materials and methods

### 2.1. Materials and reagents

Zinc acetate dihydrate, 2-methylimidazole, sodium hydroxide, 4-(2-hydroxyethyl)-1-piperazineethanesulfonic acid (HEPES), kanamycin, neomycin, streptomycin, achromycin, and gentamycin were from J&K Chemical, China, Ltd. Hydrochloric acid was purchased from local suppliers. 2,2′,2″,2‴-((ethene-1,1,2,2-tetrayltetrakis (benzene-4,1-diyl)) tetrakis (oxy)) tetraacetic acid (TPE) with 1HNMR characteristic spectra shown in Fig. S1 was a gift from Prof. Dai of Nanjing Normal University. All reagents were of analytical grade and directly used without further purification. Ultrapure water from a water purification system (18.25 MΩ cm, UPT-II-10 T, Ulu pure Corporation, China) was used in all experiments.

### 2.2. Apparatus

The fluorescence measurements were performed using an RF-5301 PC fluorescence spectrophotometer (Shimadzu, Japan). Ultraviolet–visible (UV–vis) absorption spectra were recorded using a UV 2600 spectrophotometer (Shimadzu). The transmission electron microscopy (TEM) images were taken on a Tecnai G2 F20 apparatus (FEI, USA). X-ray diffraction (XRD) patterns were acquired on a Bruker D8 Advance (Germany) diffractometer. The Fourier transform infrared (FTIR) spectrum was recorded on Thermo Scientific Nicolet 6700 in the range of 400–4000 $cm^{-1}$. The Zeta potential data were obtained by a Particle Size and Zeta Potential Analyzer (Brookhaven Instruments).

Synthesis of ZIF-8 and ZIF-8@TPE. ZIF-8 and ZIF-8@TPE were synthesized according to a reported method but with minor modification (Wang et al., 2019). In brief, 82 mg of zinc acetate dihydrate and 2 mg of TPE were added into 20 mL of *N, N*-dimethylformamide (DMF), and the mixture was stirred for 15 min. Then, 20 mL of aqueous 2-methylimidazole solution was mixed with above mixture, and the resulted solution was agitated for 6 h. Subsequently, the precipitate was subject to centrifugation (6000 rpm) for 10 min in DMF, deionized water and ethanol, separately respectively. For ZIF-8, the preparation procedure was alike that of ZIF-8@TPE. Finally, the obtained ZIF-8@TPE crystals were dispersed in HEPES buffer (10 mM, pH 7.4) and stored at 4 °C for future use (1 mg/mL).

### 2.3. Fluorescent measurement procedure for kanamycin detection

First, 2 mg of ZIF-8@TPE powder was incubated with 1 mL of HEPES buffer solution (10 mM, pH 7.4) containing 10 μM aptamers at 4 °C overnight. Then, 10 μL of kanamycin solution of a designated concentration was added to 65 μL of HEPES buffer solution, and the resulted mixture was incubated mixture for 3 h at 37 °C. After that, 10 μL of the

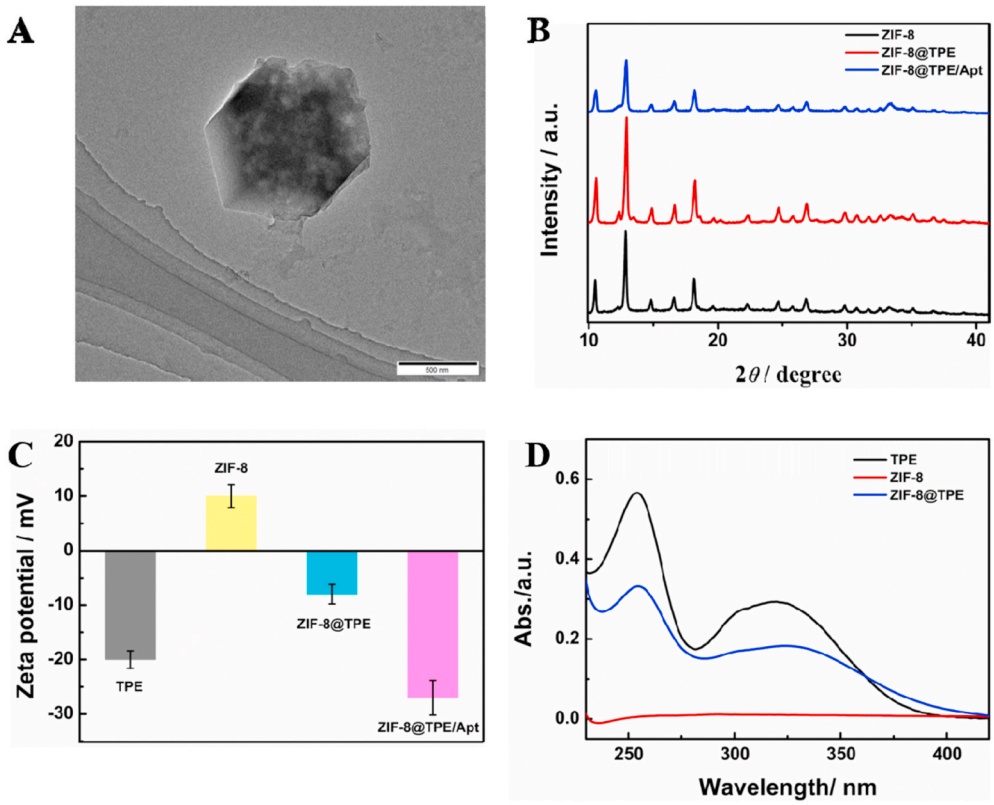


**Fig. 1.** (A) TEM image of ZIF-8@TPE, (B) XRD patterns of synthesized ZIF-8, ZIF-8@TPE and ZIF-8@TPE/Apt, (C) Zeta potential of TPE, ZIF-8, ZIF-8@TPE and ZIF-8@TPE/Apt, and (D) UV–vis absorption spectra of sole TPE, pure ZIF-8 and ZIF-8@TPE.

prepared ATP solution was dissolved into the above mixture. After 20 min, the obtained suspension was immediately transferred to a disposable cuvette for the collection of fluorescence emission spectrum in the 400–650 nm range at an excitation wavelength of 350 nm.

### 2.4. Analysis of kanamycin in real milk samples

The milk samples were purchased from a local supermarket (Huang Gang, China). First, the milk sample was subjected to centrifugation at 10,000 rpm for 20 min. Then, the upper oil and lower sediment were discarded. The supernatant was collected and filtered through 0.22 μm sterile microporous layer to obtain the milk sample. Finally, spike the kanamycin into above solution and collected the fluorescence data following the same procedures mentioned earlier.

### 2.5. Specificity

To investigate the selectivity of the proposed assay, we employed other antibodies such as streptomycin, neomycin, achromycin and gentamycin as interfering agents. To a mixture of ZIF-8@TPE/Apt, 10 μL of the assigned interfering antibody was added and incubated at 37 °C for 3 h. Then, 10 μL of ATP solution was added, and after reaction of 20 min, fluorescence emission spectrum was collected in the 400–650 nm range at an excitation wavelength of 350 nm.

## 3. Results and discussion

### 3.1. Characterization of ZIF-8@TPE

The morphology and size of the obtained ZIF-8@TPE was characterized by TEM. As exhibited in Fig. 1A, the diameter of the monodispersed ZIF-8@TPE was about 600 nm, which is consistent with the work of Wang et al., (2019). Then, X-ray diffraction (XRD) patterns were acquired to evaluate the crystalline structure of ZIF-8, ZIF-8@TPE and ZIF-8@TPE/Apt (Fig. 1B). All peaks of ZIF-8 in the range of 10°–40° match well with that of simulated single crystal of ZIF-8, suggesting successful synthesis of ZIF-8. For ZIF-8@TPE, the XRD pattern is almost identical to that of pure ZIF-8, implying that the encapsulated TPE molecules have little effect on the crystallinity of ZIF-8. With the capping of aptamers on the surface of ZIF-8@TPE via π-π stacking and electrostatic interactions, the XRD pattern of ZIF-8@TPE/Apt matches well with that of ZIF-8@TPE, indicating that the oligonucleotide has little effect on the formation of ZIF-8. Samples of the as-prepared TPE, ZIF-8 and ZIF-8@TPE were then characterized by FTIR (Fig. S2). The peaks at 3450 $cm^{-1}$ and 1705 $cm^{-1}$ in the spectrum of the TPE can be assigned to the stretching vibrations of.

The O–H bond and C═O bond, respectively, indicating the presence of carboxyl groups (Liu et al., 2018). Compared with pure ZIF-8, the peaks at 1740, 1602, 1507, 1230 and 836 $cm^{-1}$ are observed in the spectrum of ZIF-8@TPE, suggesting successful encapsulation of TPE in ZIF-8. Moreover, after the embedment of negatively charged TPE in positively charged ZIF-8, there is change of ZIF-8@TPE zeta potential from positive to negative, further confirming the successful synthesis of ZIF-8@TPE. After the introduction of aptamers on the surface of ZIF-8@TPE, the zeta potential of ZIF-8@TPE becomes more negative (Fig. 1C), which suggests the formation of ZIF-8@TPE/Apt. Fig. 1D shows the UV–vis absorption of TPE, ZIF-8 and ZIF-8@TPE. The spectrum of TPE shows obvious absorption peaks at 252 nm (B band of benzene ring) and 320 nm (n→Π* electronic transition of C═O). Compared with pristine ZIF-8, the characteristic peak of TPE emerges in the absorption spectrum of ZIF-8@TPE, which further confirms the successful fabrication of ZIF-8@TPE. Besides, after being decorated with aptamers, there is redshift of the absorption peak at 252 nm–260 nm, suggesting the existence of the aptamers (Fig. S3).

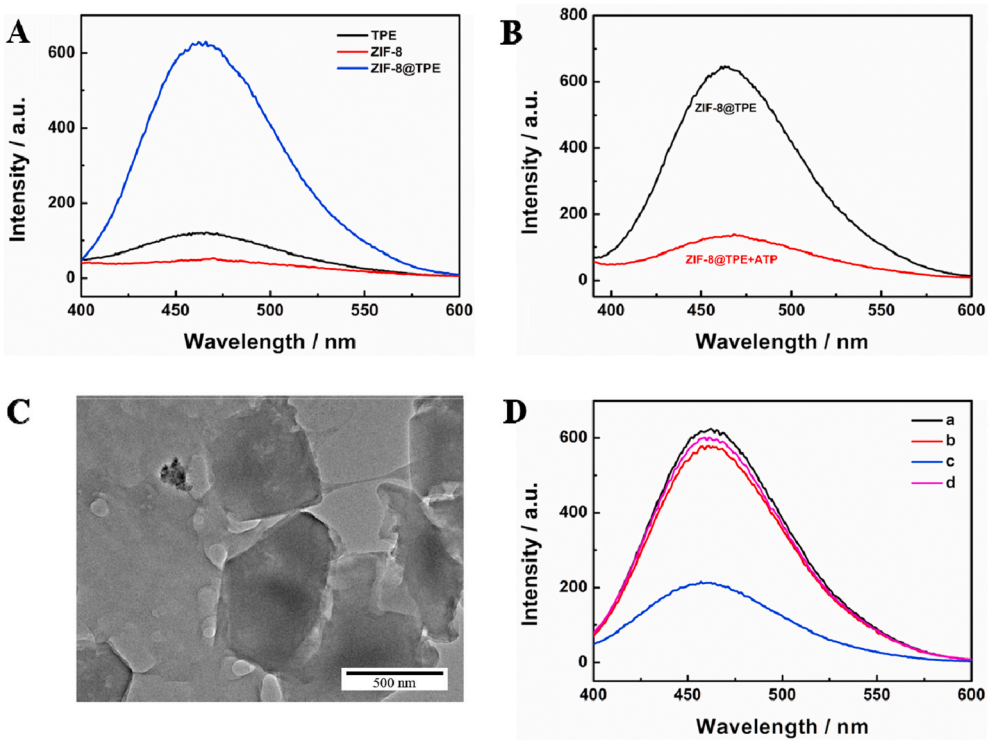


**Fig. 2.** (A) Fluorescence spectra of ZIF-8, TPE and ZIF-8@TPE. (B) Fluorescence response of ZIF-8@TPE before (black line) and after (red line) the addition of ATP (100 μM). (C) TEM image of ZIF-8@TPE after the reaction with 100 μM ATP for 10 min. (D) Fluorescence response of (a) ZIF-8@TPE/Apt, (b) ZIF-8@TPE/Apt + ATP, (c) ZIF-8@TPE/Apt + ATP + kanamycin, and (d) ZIF-8@TPE/Apt + kanamycin. (For interpretation of the references to color in this figure legend, the reader is referred to the Web version of this article.)

### 3.2. Feasibility test of the kanamycin sensing strategy

The potential of the proposed method for kanamycin detection was investigated. As show in Fig. 2A, with excitation of 360 nm, TPE by itself emits fluorescence at 460 nm. For pristine ZIF-8, the fluorescence intensity at 460 nm is extremely weak. When TPE molecules were encapsulated in ZIF-8, the fluorescence intensity increases dramatically owing to the confined state of TPE molecules, which further confirms the formation of ZIF-8@TPE. However, upon exposure to an acidic environment or to competitive ligands, the metal-organic frameworks

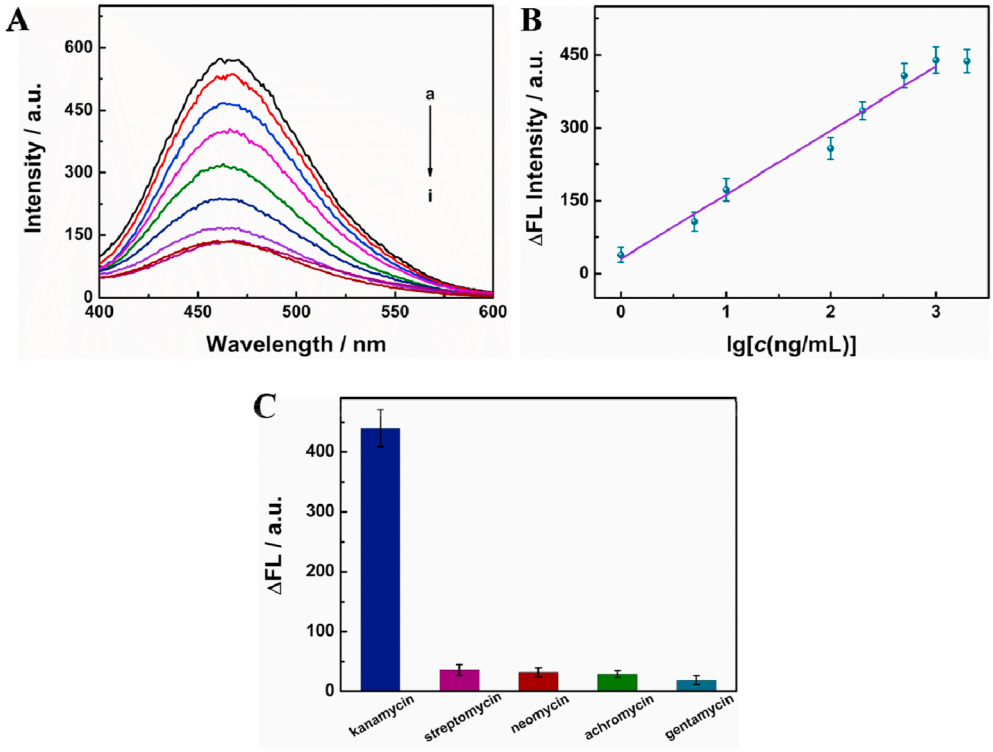


**Fig. 3.** (A) Fluorescence response of the proposed aptasensor to kanamycin with concentration varied from 0 to $10^3$ ng/mL, (B) Linear calibration curve between fluorescence change and kanamycin concentration (The error bars show the standard deviation for three independent experiments), and (C) Specificity of the constructed platform for different antibiotics (kanamycin: $10^3$ ng/mL, other antibiotics: $10^4$ ng/mL).

collapse. As show in Fig. 2B, the intense fluorescence of ZIF-8@TPE was effectively quenched after incubation with ATP for 10 min, suggesting that ATP has stronger coordination with $Zn^{2+}$ than 2-methylimidazole and could trigger the collapse of ZIF-8@TPE. As displayed in Fig. 2C, in the presence of ATP, the morphology of ZIF-8@TPE is in a form of irregular aggregation rather than neat and orderly, indicating the damage of ZIF-8 and the release of TPE. The random TPE molecules show weak fluorescence (Fig. 2B, red line). Moreover, we further investigated the collapse of ZIF-8@TPE and the release of TPE molecules by UV–vis spectroscopy. As depicted in Fig. S4, the absorption spectra of the supernatant of ZIF-8@TPE in the presence and absence of ATP were collected. respectively. The absorption peak of the supernatant of ZIF-8@TPE at 252 nm and 320 nm is weak (curve c). Upon the addition of ATP, the absorption peaks at 252 nm and 320 nm dramatically increase in intensity, validating the decomposition of ZIF-8@TPE and the release of TPE (curve d). These phenomena confirm the potential of the fabricated ZIF-8@TPE for kanamycin detection based on the fluorescence technique.

After that, we investigated the feasibility of the fabricated biosensor for kanamycin detection (Fig. 2D). The synthesized ZIF-8@TPE/Apt exhibits intense fluorescence emission due to the limited intramolecular rotation of TPE in the confined state (curve a). When ATP was added to the HEPES containing ZIF-8@TPE/Apt, there is no obvious change of fluorescence intensity, indicating that ZIF-8 remains intact (curve b). That is, the aptamers hinder the coordination of ATP to zinc ion due to electrostatic repulsion. Nonetheless, with aptamers being specifically identified and captured by kanamycin, there is its removal from ZIF-8@TPE, leaving ZIF-8@TPE at a naked state for ATP coordination, and the outcome is significant decrease of fluorescence intensity (curve c). In the absence of ATP, kanamycin alone has negligible influence on the fluorescence response of ZIF-8@TPE/Apt (curve d). These phenomena suggest that it is feasible to establish an assay for the detection of kanamycin based on fluorescence strategy.

### 3.3. Optimization of experimental conditions

As a competitive ligand, ATP has a great influence on the fluorescence of ZIF-8@TPE. With the aid of ATP, more TPE molecules randomly escaped from ZIF-8 into the HEPES buffer, and the fluorescence was weakened. When the concentration of ATP was increased from 0 to 100 μM, the fluorescence intensity decreased markedly and plateaued at 100 μM, suggesting a negative relationship between fluorescence intensity and ATP concentration (Fig. S5). Consequently, a ATP concentration of 100 μM was adopted for further optimization of the fluorescence assay.

The effects of reaction time between ATP with ZIF-8@TPE were also investigated. In the presence of ATP, the structure of ZIF-8@TPE would be destroyed, leading to robust ATP coordination with $Zn^{2+}$. As shown in Fig. S6, the fluorescence intensity decreased rapidly with the increase of reaction time and plateaued after a reaction time of 10 min. Thus, 10 min was chosen as the optimal time for the coordination reaction.

Furthermore, the incubation time for specific recognition between aptamers and kanamycin also played a critical role. Under the optimized conditions, the fluorescence intensity markedly decreased in the beginning 3 h and then leveled off, indicative of the reach of reaction equilibrium. Therefore, 3 h was adopted as the optimal incubation time for the fluorescence assay. (Fig. S7).

### 3.4. Analytical performance of the fluorescence biosensor

To evaluate the performance of the developed fluorescence assay, the fluorescence responses of ZIF-8@TPE/Apt were recorded at different kanamycin concentrations under the optimized conditions (Fig. 3A). There is gradual decrease of fluorescence intensity with increasing kanamycin concentration from 0 to $10^3$ ng/mL. The calibration curve was established by plotting ΔFL (ΔFL = $FL_0$−FL; where $FL_0$ is the intensity at zero kanamycin concentration and FL is the response at a particular kanamycin concentration) versus kanamycin concentration. The fitted linear regression equation is $\Delta FL_{465nm} = 132.07 \times lgC + 30.62$ (ng/mL) with a correlation coefficient of 0.984. The detection limit was estimated to be 7.3 ng/mL at 3σ criterion, which is comparable to those of literatures shown in Table S1. The excellent analytical performance may be attributed to the efficient specific Apt-target reaction and strong ATP coordination ability with zinc ion.

**Table 1**
Detection of kanamycin in milk samples.

| Sample | Spink amount (ng/mL) | Detected (ng/mL) | Recovery (%) |
|---|---|---|---|
| 1 | 0 | 2.2 | / |
| 2 | 100 | 86.1 | 86.1 |
| 3 | 500 | 543.3 | 108.7 |
| 4 | 1000 | 914 | 91.4 |

### 3.5. Specificity of proposed platform

To investigate the specificity of the developed biosensor, the fluorescence of ZIF-8@TPE/Apt in the presence of analogous antibiotics including streptomycin, neomycin, achromycin, and gentamycin were tested under the optimized conditions. As shown in Fig. 3C, only kanamycin could significantly affect the fluorescence signal of ZIF-8@TPE/Apt and the others have relatively less effect, demonstrating the excellent selectivity of the fabricated assay for kanamycin detection. In other words, the analogous antibiotics fail to recognize the kanamycin-related aptamers and the ZIF-8@TPE remains intact.

### 3.6. Real sample analysis

To evaluate the applicability of the proposed assay with a real sample, HEPES diluted standard milk samples were spiked with various concentrations of kanamycin and tested at the optimized conditions. As shown in Table 1, the recovery of the samples ranges from 86.1% to 108.7%. The results indicate that the designed assay is practically applicable for kanamycin detection.

## 4. Conclusion

In conclusion, a novel label-free fluorescent aptasensor has been developed for the detection of kanamycin (Kana) by utilizing ZIF-8@TPE as fluorophore and aptamer as recognition unit. The fluorescence of ZIF-8@TPE could be quenched by ATP via competitive coordination reactions. Taking advantage of the conformational change of Kana-aptamer capped on ZIF-8@TPE before and after binding with the target kanamycin, the monitor of kanamycin can be realized with superior sensitivity. This assay has a wide linear range, as well as low detection limit and good specificity for kanamycin detection. Moreover, by altering the aptamer sequence, the reported strategy provides a feasible way for sensitive detection of other antibiotics for analysis of food samples.

## Declaration of competing interest

The authors declare that they have no known competing financial interests or personal relationships that could have appeared to influence the work reported in this paper.

## Acknowledgements

This work was supported by the National Natural Science Foundation of China (22004044), Hubei Province Natural Science Foundation (2020CFB426), Doctoral Fund Project of Huanggang Normal University (2042019027), and Research Foundation of Huanggang Normal University (204201913103). The authors thank Prof. C.T. Au for helpful

suggestions.

## Appendix A. Supplementary data

Supplementary data to this article can be found online at https://doi.org/10.1016/j.envres.2021.112617.

## References


Ben, Y., et al., 2019. Human health risk assessment of antibiotic resistance associated with antibiotic residues in the environment: a review. Environ. Res. 169, 483–493.

Cai, X., et al., 2017. Aggregation-induced emission luminogen-based direct visualization of concentration gradient inside an evaporating binary sessile droplet. ACS Appl. Mater. Interfaces 9, 29157–29166.

Chen, Y., et al., 2009. LC method for the analysis of kanamycin residue in swine tissues using derivatization with 9-fluorenylmethyl chloroformate. J. Separ. Sci. 29, 3620–3626.

Chen, X.X., et al., 2018. A microchip electrophoresis-based assay for ratiometric detection of kanamycin by R-shape probe and exonuclease-assisted signal amplification. Talanta 189, 494–501.

Cheng, S.T., et al., 2020. Highly sensitive electrochemiluminescence aptasensor based on dual-signal amplification strategy for kanamycin detection. Sci. Total Environ. 737, 139785.

Feng, J.L., et al., 2018. Detection of listeria monocytogenes based on combined aptamers magnetic capture and loop-mediated isothermal amplification. Food Control 85, 443–452.

Gu, C.C., et al., 2021. Highly sensitive and stable self-powered biosensing for exosomes based on dual metal-organic frameworks nanocarriers. Biosens. Bioelectron. 176, 112907.

Gu, C.C., et al., 2019. Enzymatic biofuel-cell-based self-powered biosensor integrated with DNA amplification strategy for ultrasensitive detection of single-nucleotide polymorphism. Anal. Chem. 91, 8697–8704.

He, L., et al., 2019. A microfluidic chip based ratiometric aptasensor for antibiotic detection in foods using stir bar assisted sorptive extraction and rolling circle amplification. Analyst 144, 2755–2764.

He, J.X., et al., 2016. Preparation of artificial antigen and development of IgY-based indirect competitive ELISA for the detection of kanamycin residues. Food Anal. Methods 9, 744–751.

Hou, Y.-H., et al., 2018. A colorimetric and electrochemical immunosensor for point-of-care detection of enterovirus 71. Biosens. Bioelectron. 99, 186–192.

Jiang, Y., et al., 2018. Surface enhanced Raman spectroscopy (SERS): a novel reliable technique for rapid detection of common harmful chemical residues. Trends Food Sci. Technol. 75, 10–22.

Jiang, Y., et al., 2019. Ultrasensitive analysis of kanamycin residue in milk by SERS-based aptasensor. Talanta 197, 151–158.

Kuehn, B., et al., 2019. Antibiotic resistance threat grows. J. Am. Med. Assoc. 322, 2376.

Lan, L.Y., et al., 2017. Recent advances in nanomaterial-based biosensors for antibiotics detection. Biosens. Bioelectron. 91, 504–514.

Li, Y.H., et al., 2019. Creation of efficient blue aggregation-induced emission luminogens for high-performance nondoped blue OLEDs and hybrid white OLEDs. ACS Appl. Mater. Interfaces 11, 17592–17601.

Liang, K., et al., 2015. Biomimetic mineralization of metal-organic frameworks as protective coatings for biomacromolecules. Nat. Com. 6, 7240.

Liu, Y.Z., et al., 2020. Tuning biosensor cross-reactivity using aptamer mixture. Anal. Chem. 92, 5041–5047.

Liu, S.S., et al., 2018. Green light excited ultrasensitive photoelectrochemical biosensing for microRNA at a low applied potential based on the dual role of Au NPs in $TiO_2$ nanorods/Au NPs composites. Nanoscale 10, 16474–16478.

Ma, H.J., et al., 2021. Multifunctional organic fluorescent probe with aggregation-induced emission characteristics: ultrafast tumor monitoring, two-photon imaging, and image-guide photodynamic therapy. ACS Appl. Mater. Interfaces 13, 7987–7996.

Peng, W.P., et al., 2020. Nonenzyme cascaded amplification biosensor based on effective aggregation luminescence caused by disintegration of silver nanoparticles. ACS Sens. 7, 1912–1920.

Preu, M., et al., 1998. Development of a gas chromatography-mass spectrometry method for the analysis of aminoglycoside antibiotics using experimental design for the optimisation of the derivatisation reactions. J. Chromatogr. A 818, 95–108.

Qu, L.L., et al., 2016. Highly reproducible Ag NPs/CNT-intercalated GO membranes for enrichment and SERS detection of antibiotics. ACS Appl. Mater. Interfaces 8, 28180–28186.

Ramezani, M., et al., 2016. A selective and sensitive fluorescent aptasensor for detection of kanamycin based on catalytic recycling activity of exonuclease III and gold nanoparticles. Sens. Actuators, B 222, 1–7.

Shi, L.X., et al., 2020. In situ biomimetic mineralization on ZIF-8 for smart drug delivery. ACS Biomater. Sci. Eng. 6, 4595–4603.

Son, S.U., et al., 2019. Naked-eye detection of pandemic influenza a (pH1N1) virus by polydiacetylene (PDA)-based paper sensor as a point-of-care diagnostic platform. Sens. Actuators B Chem. 291, 257–265.

Tian, L., et al., 2020. Ratiometric dual signal-enhancing-based electrochemical biosensor for ultrasensitive kanamycin detection. Sci. Total Environ. 12, 52713–52720.

Wang, X.R., et al., 2014. Highly selective fluorogenic multianalyte biosensors constructed via enzyme-catalyzed coupling and aggregation-induced emission. J. Am. Chem. Soc. 136, 9890–9893.

Wang, L.M., et al., 2020. Integrating target-triggered aptamer-capped HRP@metal−organic frameworks with a colorimeter readout for on-site sensitive detection of antibiotics. Anal. Chem. 92, 14259–14266.

Wang, L., et al., 2019a. HRP@ZIF-8/DNA hybrids: functionality integration of ZIF-8 via biomineralization and surface absorption. ACS Sustain. Chem. Eng. 7, 14611–14620.

Wang, T.T., et al., 2019b. Electrochemical aptasensor for ampicillin detection based on the protective effect of aptamer-antibiotic conjugate towards DpnII and Exo III digestion. Talanta 197, 42–48.

Xi, X.G., et al., 2021. Label-free quartz crystal microbalance biosensor based on aptamer-capped gold nanocages loaded with polyamidoamine for thrombin detection. ACS Appl. Nano Mater. 4, 10047–10054.

Yan, Z.D., et al., 2016. A sensitive electrochemical aptasensor for multiplex antibiotics detection based on high-capacity magnetic hollow porous nanotracers coupling exonuclease-assisted cascade target recycling. Biosens. Bioelectron. 78, 51–57.

Yao, Y., et al., 2019. Flexible freestanding graphene paper-based potentiometric enzymatic aptasensor for ultrasensitive wireless detection of kanamycin. Biosens. Bioelectron. 123, 178–184.

Zeng, R.J., et al., 2021. Photoelectrochemical bioanalysis of antibiotics on rGO-Bi2WO6-Au based on branched hybridization chain reaction. Biosens. Bioelectron. 133, 100–106.

Zeng, X., et al., 2019. Highly efficient deep blue aggregation-induced emission organic molecule: a promising multifunctional electroluminescence material for blue/green/orange/red/white OLEDs with superior efficiency and low roll-off. ACS Photonics 6, 767–778.

Zhang, Y., et al., 2020. Dual triple helix-aptamer probes for mix-and-read detecting antibiotics in fish and milk. J. Agric. Food Chem. 68, 9524–9529.

Zhou, Y.Y., et al., 2020. Development of fluorescent aptasensing system for ultrasensitive analysis of kanamycin. J. Lumin. 222, 117124.

Zhou, Y.L., et al., 2019. Electrochemical aptasensing strategy for kanamycin detection based on target-triggered single-strand DNA adsorption on $MoS_2$ nanosheets and enzymatic signal amplification. Sens. Actuators B Chem. 296, 126664.